

# Multi-objective optimization of transesterification in biodiesel production catalyzed by immobilized lipase

Mahmoud Karimi, Arak University, Iran and Stanford University, CA, USA  
Bryan Jenkins and Pieter Stroeve, University of California Davis, CA, USA

Received December 15, 2015; revised July 24, 2016; and accepted July 25, 2016  
View online September 14, 2016 at Wiley Online Library (wileyonlinelibrary.com);  
DOI: 10.1002/bbb.1706; *Biofuels, Bioprod. Bioref.* 10:804–818 (2016)

**Abstract:** In order to comply with criteria of green energy concepts and sustainability, a multi-objective analysis was performed for the transesterification of waste cooking oil (WCO) using immobilized lipase. Response surface methodology and artificial neural networks, followed by multiple response optimization through a desirability function approach were applied to individually and simultaneously evaluate the fatty acid methyl esters (FAME) content and the exergy efficiency. Reaction time and concentrations of methanol, immobilized lipase and water were considered as the design variables in maximizing FAME content and exergy efficiency. The maximum individual desirability of FAME content was predicted to be 95.7% corresponding to a methanol to WCO molar ratio of 6.7, catalyst concentration of 45%, water content of 9% and reaction time of 25 h. However, based on the simultaneously optimization of both the FAME content and the exergy efficiency, the maximum overall desirability was found at a methanol to WCO molar ratio of 6.7, catalyst concentration of 35%, water content of 12% and reaction time of 20 h to achieve FAME content of 88.6% and exergy efficiency of 80.1%, respectively. © 2016 Society of Chemical Industry and John Wiley & Sons, Ltd

**Keywords:** thermodynamic analysis; enzymatic transesterification; lipase immobilization; optimization; biodiesel; exergy

## Introduction

Limited energy reserves and increasing environmental pressure on greenhouse gases (GHGs) from fossil fuels has caused biodiesel (fatty acid alkyl esters) to become a topic of interest in and target of energy policy in many countries.<sup>1,2</sup> Biodiesel has drawn attention in the last decade as a low toxicity, biodegradable, renewable source

of fuel with generally lower exhaust emissions and reduced lifecycle GHG implications for CO, CO<sub>2</sub> and SO<sub>x</sub> in comparison with petroleum fuels. Therefore biodiesel is mostly considered an environmentally friendly alternative liquid fuel and energy product.<sup>1,3</sup>

Biodiesel is produced by esterification of fatty acids or transesterification of triglycerides with short chain alcohols like methanol and ethanol. Methanol is mostly used

because of its lower cost compared with other alcohols, so biodiesel most commonly refers to fatty acid methyl esters (FAME). However, one of the major obstacles to wide application of biodiesel is its high cost in comparison of fossil diesel.<sup>4</sup> It has been reported that the cost of raw materials amounts to around 75% of the total biodiesel production cost.<sup>5</sup> Therefore, sustainability of biodiesel production depends on low cost feedstock such as waste cooking oil (WCO) to reduce the overall cost of biodiesel production.<sup>6</sup>

Biodiesel can be synthesized chemically or enzymatically according to the catalysts employed in the process. Short time and high yields are considered to be advantages of chemical transesterification versus drawbacks such as high energy requirements, difficulties in the recovery of the catalyst and coproduct glycerol and potential pollution of the environment associated with alkali or acid catalyzed processes.<sup>2,7</sup> Lipase has attracted the attention of researchers as a biocatalyst with fewer disadvantages compared to chemical transesterification.<sup>8</sup> The high cost of lipase has been recognized as the main obstacle for industrial application of biocatalyst in transesterification. Immobilization methods have been introduced to produce immobilized lipase and improve lipase stability and allow for repeated utilization.<sup>2,9,10</sup>

Another point to be considered is the efficiency of biodiesel production measured in terms of both the first and the second laws of thermodynamics. Producing a renewable energy source usually involves the consumption of non-renewable resources. When the exergy content of a non-renewable resource is altered through an irreversible process, the environment is also considered altered. Hence, much research<sup>11–13</sup> has been undertaken on the exergy accounting of non-renewable resource consumption in order to measure the environmental impact of many manufacturing processes. The intensive exploitation of a renewable energy source may also cause a destruction of exergy through excessive wastes due to insufficient materials recycling. Some work and non-renewable resources are needed to treat these wastes in order to reduce or prevent environmental damage.<sup>13,14</sup>

Most real processes need to be optimized with respect to several criteria simultaneously. Frequently, design or operating conditions are constrained for meeting product specifications. Sustainable enzymatic biodiesel production, for example, needs to be optimized both in terms of yield efficiency and exergy destruction. Exergy-based criteria were found to give much better guidance for system improvement, as they account better for use of energy resources. However, one of the most important reasons

in this field also is net energy yield through biodiesel. Therefore the system needs to be improved through both the reduction of exergy destruction and the enhancement of biodiesel yield, simultaneously. There are different methods to optimize operating conditions such as the conventional graph method,<sup>15</sup> improved graph method,<sup>16</sup> desirability functions,<sup>17</sup> the extended surface procedure,<sup>18</sup> response surface methodology (RSM),<sup>19</sup> and artificial neural networks (ANN).<sup>20</sup>

RSM has important applications in research and industry for the design and development of new products and the improvement of existing products. RSM defines the effect of the controlling independent variables, alone or in combination, on the process response. The methodology employs mathematical models describing the industrial process.<sup>19</sup> However RSM may not be applicable to optimize for all processes although it has many advantages. RSM can only develop first-degree and second-degree models that is considered as a disadvantage of this technique for data that could be fitted better on other models.

ANN have been used in many fields of science, engineering, and medicine due to their utility in solving non-linear problems.<sup>20</sup> Neural networks are useful when exact mathematical information is not available. Another advantage of ANN models over rule-based models is the potential to add new data for retraining the network, if the process under analysis changes. This typically is much easier than determining new models or rules. ANN models are at a disadvantage compared to rule-based modeling, like RSM, for explaining the relationship between independent and dependent variables because of using ambiguously defined weights.

Due to the high surface area of mesoporous silica which can increase the immobilization density as well as the property of superparamagnetic iron oxide nanoparticles (SPION), which helps the recovery of lipase, the mesoporous silica–SPION core-shell (Fe<sub>3</sub>O<sub>4</sub> at SiO<sub>2</sub>) was produced as a promising candidate for immobilization of *T. lanuginosa* on lipase in the present work. This research focused on modeling the following influences on the FAME content and exergy efficiency of the transesterification of WCO: molar ratio of methanol to WCO ( $m$ ), weight percent of immobilized lipase to WCO ( $l$ ), water content ( $w$ ), and reaction time ( $t$ ). This study has been carried out with the aim of providing information on the operating conditions that provide the best FAME content while also having the least material and energy requirements through minimizing exergy losses by using two techniques of the response surface methodology and the artificial neural network.

## Materials and methods

### Materials

Food grade cooking canola oil was purchased retail and then used in frying potatoes and finally collected and stored in a glass container at room temperature. The physicochemical properties of the WCO including density, viscosity, free fatty acid (FFA) content, and acid value were 0.906 g/cm<sup>3</sup>, 51.3 cP, 5.68%, and 11.16, respectively. The density and viscosity of oil were measured by a pycnometer and a viscometer, respectively, whereas the FFA content and acid values were determined by acid–base titration. Methanol, ethanol, pellets of sodium hydroxide (97%), hydrochloric acid (36.5–38%), ammonium hydroxide (28–30% NH<sub>3</sub> basis), ferric chloride hexahydrate (98%), ferrous chloride tetrahydrate (99%), tetramethyl ammonium hydroxide (25%), hexadecyltrimethyl ammonium bromide (CTAB; 99%), tetraethylorthosilicate (TEOS; 98%), dimethyloctadecyl[3-(trimethoxysilyl)propyl] ammonium chloride (72%), and *Thermomyces lanuginose* lipase with activity >10<sup>5</sup> units/g were all purchased from Sigma–Aldrich, St. Louis, MO, USA. All reagents were used as received without further purification. Deionized water was used in all experiments.

### Preparation of magnetic nanoparticles

Superparamagnetic mesoporous silica-SPION core-shell nanoparticles (NPs) were prepared based on the method described in the previous work.<sup>2</sup> The SPIONs were produced by coprecipitation of degasified and acidic ferric chloride hexahydrate (10.81 g) and ferrous chloride tetrahydrate (3.97 g) in ammonium hydroxide (0.7 M) in a round-bottom flask reactor under bubble nitrogen gas and magnetic stirring. The prepared ferrofluid solution was kept at 4°C under N<sub>2</sub> atmosphere until further use for core generation in magnetic NPs.

The mesoporous silica/iron oxide superparamagnetic core-shell NPs were prepared based on a sol–gel method by using tetraethylorthosilicate (TEOS) as the precursor and hexadecyltrimethyl ammonium bromide (CTAB) as the dispersant, pore formation, and capping agent. The particles were then separated using a magnet and washed several times. The magnetic NPs were finally oven dried at 70–80°C for 12 h, then calcined at 550°C for 8 h. The magnetic properties and surface area have been reported in our previous report.<sup>21</sup>

### Immobilization of lipase

In order to immobilize lipase onto magnetic NPs, the functional groups of microspheres were activated using

dimethyloctadecyl [3-(trimethoxysilyl) propyl] ammonium chloride coupling agent for a linkage with the amino acid residue of lipase.<sup>22,23</sup> Lipase can be covalently immobilized on the superparamagnetic nanoparticles by forming a Schiff base linkage between the alkyl group of dimethyloctadecyl [3-(trimethoxysilyl) propyl] ammonium chloride and the terminal amino group of lipase. For this purpose, 10 g of dried magnetic NPs were re-dispersed in 100 mL of ethanol (95%) and 150 mL of glycerol and subsequently stirred at 600 rpm for 10 min. About 10 mL of dimethyloctadecyl [3-(trimethoxysilyl) propyl] ammonium chloride (72%) was vigorously added to the mixture and the reaction was heated to 85°C in a silicon oil bath and stirred at 750 rpm for 12 h. The alkyl-grafted SPION-silica NPs were decanted by a magnetic device and washed with ethanol several times to completely remove unadsorbed components. Then, the particles were dried at 100°C for 24 h in a thermal oven and stored at ambient conditions until further use.

A typical immobilization was then started with re-dispersion of 10 g of the alkyl-grafted NPs in ethanol (99.9%) and then decanted by the magnetic device. The *T. lanuginose* lipase was added at an enzyme weight to solution volume ratio of 2 (w/v) under vigorous mechanical stirring at 30°C for 6 h. The immobilized lipase was then decanted by an external magnetic field and washed with deionized water for several times until complete removal of the unbound lipase. The immobilized lipase was finally dried by lyophilization at –50°C and 25 kPa for 48 h.

### Enzymatic transesterification

In the first step of enzymatic transesterification, waste oil was vacuum-filtered with filter paper to remove impurities. The refined WCO was heated to 80°C and continuously stirred for 10 min with 1% of H<sub>3</sub>PO<sub>4</sub> (85%). The mixture was then centrifuged to completely remove the contents of colloid and water inside the refined WCO. Transesterification reactions were performed in 50 cm<sup>3</sup> capped flasks on a shaking incubator. A typical reaction mixture included 5 g WCO, 500 mg *n*-hexane, pre-determined methanol/oil molar ratio, immobilized lipase concentration and water content. Methanol was added to the reaction through three-step addition with equal amount and time interval in each step. After finishing the pre-determined times of reaction, the reaction mixtures were carefully filtered by magnetic separation. The excess methanol of each sample was distilled with the help of a rotary evaporator under reduced pressure, and then the samples were taken under room temperature to measure the FAME content.

## FAME assay

The FAME contents in the samples were analyzed by gas chromatography (Shimadzu GC-2010) equipped with a hydrogen flame ionization detector. The separation was carried out on a DB-1HT capillary column (30 m × 0.25 mm). The GC was calibrated by methyl salicylate, methyl palmitate, methyl stearate, methyl oleate, methyl linoleate and methyl linoleate, under various concentrations. During the analysis, the temperature of the sampling inlet was 370 °C and detector temperature was 375 °C. The temperature was initially maintained at 150 °C for 2 min, then raised to 360 °C at a rate of 10 °C min<sup>-1</sup> and maintained for 10 min. The carrier gas was nitrogen at a pre-column pressure of 100 kPa. The FAME content in the samples was calculated by the following equation:

$$X(\%) = \frac{m_{\text{FAME}}}{m_{\text{CB}}} \times 100\% \quad (1)$$

where  $X$  is the FAME content,  $m_{\text{FAME}}$  is the weight of FAME calculated with internal calibration method, and  $m_{\text{CB}}$  is the weight of the crude biodiesel.<sup>24</sup>

## Exergy analysis

Four balance equations must be applied for a general steady state (no accumulation) in order to find the work and heat interactions. Mass input and output is always balanced according to the principle of mass conservation given by Eqn (2). Energy input and output are also balanced at steady state according to the first law of thermodynamics or the energy conservation principle given by Eqn (3). According to the second law of thermodynamics, in real processes entropy increases as given by Eqn (4) and a part of the exergy input is always destroyed as given by Eqn (5).

$$\sum_i (\dot{m}_i)_{\text{in}} = \sum_i (\dot{m}_i)_{\text{out}} \quad (2)$$

$$\sum_i (\dot{m}_i \times h_i)_{\text{in}} = \sum_i (\dot{m}_i \times h_i)_{\text{out}} + \dot{Q} - \dot{W} = 0 \quad (3)$$

$$\sum_i (\dot{m}_i \times s_i)_{\text{in}} = \sum_i (\dot{m}_i \times s_i)_{\text{out}} + \sum_i \frac{\dot{Q}_i}{T_i} = \dot{S}_{\text{gen}} \quad (4)$$

$$\dot{e}_{\text{mass,in}} - \dot{e}_{\text{mass,out}} + \dot{e}_{\text{heat}} - \dot{e}_{\text{work}} = \dot{e}_{\text{loss}} \quad (5)$$

The mass exergy component is divided into four specific components including chemical, physical, potential and kinetic exergy expressed in Eqn (6). The potential and kinetic terms of exergy are negligible and their contribution to the total exergy balance is minimal. The physical exergy is dependent on temperature, enthalpy and entropy as shown by Eqn (7). The chemical exergy of each com-

pound is calculated by Eqn (8) which is a function of the chemical exergy of each elemental compound, the number of atoms of each element contained in the stream and the Gibbs free energy of formation for the compound.<sup>25</sup> Based on exergy balance, the exergy transfer by heat flow at a temperature  $T$  and exergy by work flow were calculated by Eqns (9) and (10), respectively,<sup>26,27</sup>

$$\dot{e}_{\text{mass}} = \dot{e}_{\text{phy}} + \dot{e}_{\text{ch}} + \dot{e}_{\text{pot}} + \dot{e}_{\text{kin}} \quad (6)$$

$$\dot{e}_{\text{phy}} = (\dot{h} - \dot{h}_0) - T_0 \times (\dot{s} - \dot{s}_0) \quad (7)$$

$$e_{\text{ch}}^0 = \Delta G_f^0 + \sum_i n_{\text{elem}} \times e_{\text{ch},i}^0 \quad (8)$$

$$\dot{e}_{\text{heat}} = \left(1 - \frac{T_0}{T}\right) \times \dot{Q} \quad (9)$$

$$\dot{e}_{\text{work}} = \dot{W} \quad (10)$$

A global mass balance across the reaction was performed, and the thermodynamic properties needed to develop the exergy balance were then obtained.<sup>28</sup> Chemical and physical exergies of input and output involved in the enzymatic transesterification of WCO were calculated. Exergy was determined for each compound, mixture and utility. Dead state conditions were taken as 298 K and 101.325 kPa with the exergy efficiency of each experiment related to the transesterification calculated using the following equation:

$$\eta = 1 - \left(\frac{e_{\text{loss}}}{e_{\text{input}}}\right) \quad (11)$$

## Design of experiment based on RSM

RSM was used to investigate the influence of the experiment variables consisting of the molar ratio of methanol to WCO ( $m$ ), immobilized lipase concentration ( $l$ ), water content ( $w$ ) and reaction time ( $t$ ) on the FAME content and exergy efficiency of the enzymatic transesterification of WCO. A four-factor-five-level rotatable central composite design (RCCD) was used in these modeling and optimization studies, which generated 27 experimental runs that were subsequently carried out. Table 1 summarizes the range and levels of the experiment variables investigated in the present study in the coded and uncoded forms.

Empirical second-order polynomial models, developed by RSM, correlate the FAME content and exergy efficiency of the in-situ transesterification as functions of the experiment variables and their interactions as shown in the following equation:

$$Y_k = \beta_0 + \sum_{i=1}^4 \beta_i x_i + \sum_{i=1}^4 \beta_{ii} x_i^2 + \sum_{i=1}^3 \sum_{j=i+1}^4 \beta_{ij} x_i x_j \quad (12)$$

**Table 1. Constraints of process variables and the respective levels for RCCD.**

Variables	Symbol coded	Range and levels				
		-2	-1	0	1	2
Methanol to WCO molar ratio	<i>m</i>	4	5	6	7	8
Immobilized lipase concentration (wt.%)	<i>l</i>	5	15	25	35	45
Water content (wt.%)	<i>w</i>	4	8	12	16	20
Reaction time (h)	<i>t</i>	5	10	15	20	25

where  $Y_k$  ( $k = 1$  and  $2$ ) are the predicted responses (FAME content and exergy efficiency),  $x_i$  is the  $i^{\text{th}}$  experiment variable,  $\beta_0$  is the intercept,  $\beta_i$  is the first order model coefficient,  $\beta_{ii}$  is the quadratic coefficient of variable  $i$  and  $\beta_{ij}$  is the interaction coefficient of variables  $i$  and  $j$ . The coefficient parameters of the developed model by RSM were estimated by multiple linear regression analysis based on least-squares and statistically evaluated by analysis of variance (ANOVA). The developed model was qualitatively evaluated by the value of correlation coefficient ( $R^2$ ) using SAS software version 9.2.

## ANN modeling

In the artificial neural network modeling, MATLAB 7.11 software was used for training and validation of neural network models. Multiple input and multiple output (MIMO) network models were developed for the experiment variables including methanol to WCO molar ratio, immobilized lipase concentration, water content and reaction time as the input layer with the responses including the FAME content and exergy efficiency of the enzymatic transesterification as the output layer of the network. A standard Bayesian regularization back propagation training algorithm, the trainer function, was employed for training the network. This training function updates the weight and bias values according to the Levenberg–Marquardt algorithm which is one of the best algorithms to improve generalization performance of neural network for function approximation problems. This is because the algorithm does not require that a validation data set be separated out of the training data set. This advantage is especially noticeable when the size of the data set is small such as is the case of the present study. The algorithm minimizes a linear combination of squared errors and weights and then determines the correct combination to produce ANN that generalizes well.<sup>19</sup>

Figure 1 shows a schematic of the network architecture developed in this study that consists of an input layer with

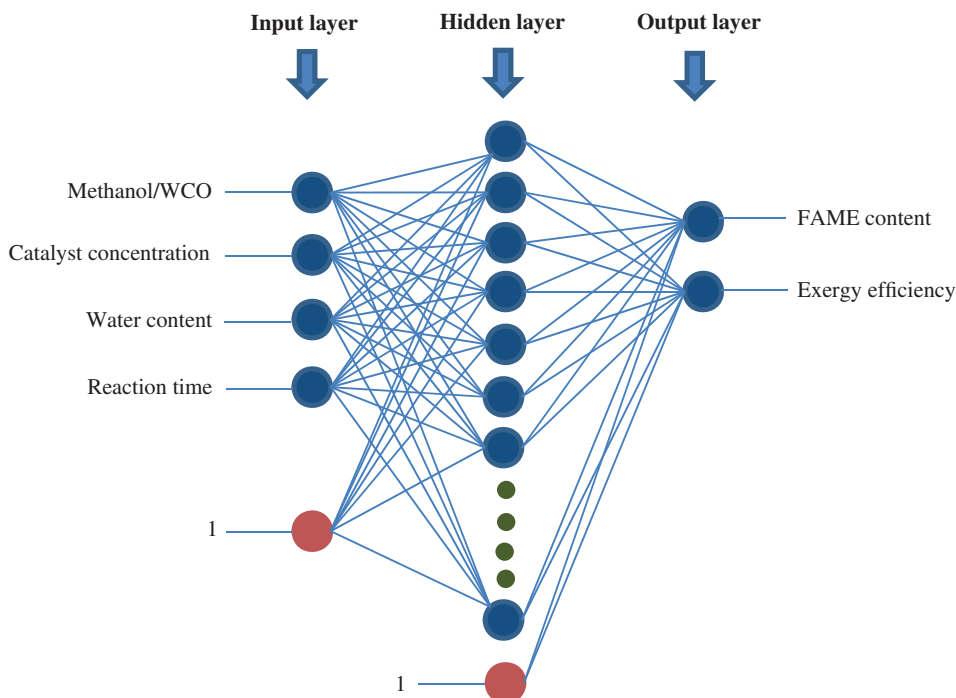


Figure 1. Schematic representation of the multilayer artificial neural network used in the present study.

four neurons, an output layer with two neurons, and a hidden layer. A total of 27 experiments were used to develop the neural network mode with 23 points used for training, 2 points for validation, and 2 points for testing. To determine the optimal network configuration, the number of neurons in the hidden layer was determined by developing several networks that vary only with the size of the hidden layer and simultaneously observing the change in the mean squared errors (MSE). The final number of neurons for this layer was 14. The optimum configuration was decided based on minimizing the difference between the neural network prediction and the desired output.

## Optimization

The desirability function approach (DFA) is one of the most widely used methods in industry for dealing with the optimization of multiple response processes. RSM is a sequential strategy which enables us to approach the optimal region and depict the response efficiently, while the desirability function approach is a useful technique for analyzing experiments in which the response needs to be optimized. RSM and DFA have been demonstrated to be efficient to optimize experiment parameters for surface roughness.<sup>19</sup> Single response optimization determines how input parameters affect the desirability of an individual response, whereas the numerical optimization finds a point that maximizes the desirability function.

Adjusting the weight or importance can alter the characteristics of a goal. The desirability function approach is first to convert each response,  $Y_k$ , into an individual desirability,  $d_k$ . The desirability scale ranges from 0 to 1, where if the response variable is outside an acceptable range,  $d_k = 0$ , and if the response is at its goal or target and fully desir-

able,  $d_k = 1$ .<sup>29</sup> Considering the situation in the enzymatic transesterification of WCO, the target for all responses (FAME content and exergy efficiency) was found to be as high as possible. Thus, a one-sided transformation was applied as:

$$d_k = \begin{cases} 1 & Y_k \geq T \\ \left(\frac{U_k - Y_k}{U_k - T_k}\right)^r & T \geq Y_k \geq U \\ 0 & Y_k \leq U \end{cases} \quad (13)$$

where  $U$  is the minimum acceptable value,  $T$  is the maximum value that is considered desirable (target value),  $Y_k$  is the response and  $r$  is the weight. The individual desirabilities were then combined using the geometric mean, which gives the overall desirability ( $D$ ):

$$D = (d_1 \times d_2)^{1/2} \quad (14)$$

Note that if any response  $k$  is completely undesirable,  $d_k = 0$  and the overall desirability will be zero.

## Results and discussion

### Characteristics of SPION-silica NPs

Figure 2 shows the typical TEM micrographs for SPION-silica NPs produced in this work. As can be seen, the magnetic NPs of  $Fe_3O_4$  have an average size of around 20 nm and the average size of the core-shell NPs is around 100 nm. The mesoporous structure of the silica can also be observed in Fig. 2. The SPION-silica NPs could be dispersed easily in water and their superparamagnetic properties prevent them from having magnetic hysteresis, which can result in agglomeration. Both the small size and the mesoporous structure of silica enhanced their active surface for immobilization and adsorption.

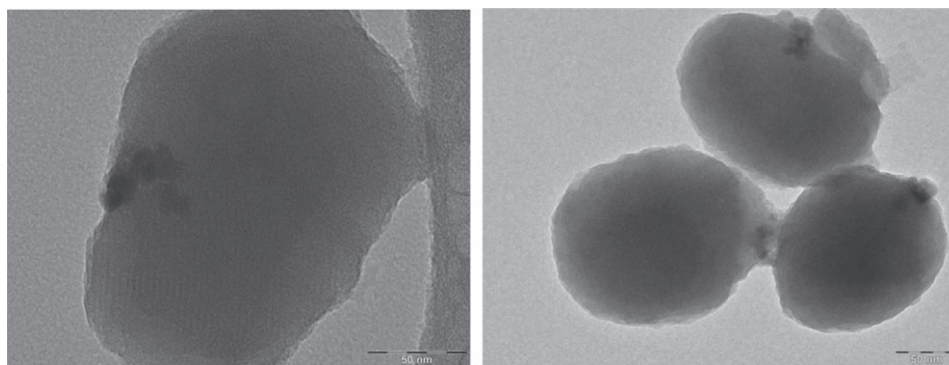


Figure 2. TEM images of SPION-silica NPs. The dark areas are the SPIONs which are embedded inside the porous silica. The nanoporous structure of the silica shell can be observed at the edges.

## Product analysis

The main components in the WCO-derived biodiesel through the enzymatic transesterification were methyl palmitate, methyl stearate, methyl oleate, methyl linoleate, methyl linoleate and methyl oleate. The methyl esters in each sample were then quantified based on the ratio of the areas under the peaks of each methyl ester to the internal standard and the known concentration of internal standard. The FAME content was calculated as the weight% of methyl ester produced over the amount of glycerides used for reaction.

## Identifying material wastes and exergy loss

The internal exergy destruction (which is unavoidable but can be minimized) for the process of enzymatic biodiesel production, including production of SPIONs, core-shell NPs, alkyl grafted core-shell NPs, immobilized lipase on the NPs, and finally the enzymatic transesterification of samples was calculated by deducting the total exergy output ( $e_{out}$ ) from the total exergy input ( $e_{in}$ ) in each step.<sup>30,31</sup> The external exergy destruction (which is avoidable) is equal to the sum of the exergy of all waste streams in the process of enzymatic biodiesel production. The overall mass and exergy balance of the enzymatic transesterification process in the coded zero condition with methanol to WCO molar ratio of 6, immobilized lipase concentration of 25%, water content of 12% and reaction time of 15 h is shown in Fig. 3. For these conditions, total input and output exergy of the enzymatic transesterification of WCO to produce 1 kg biodiesel were found to be 294.8 MJ and

278.1 MJ. The internal exergy destruction was calculated to be about 16.7 MJ per kg biodiesel production. The external waste exergy, which was assumed to be 20% of the output streams including glycerides, methanol, *n*-hexane and immobilized lipase, was equal to 38.2 MJ per kg biodiesel production.

The huge exergy destroyed in the enzymatic transesterification of WCO using the immobilized lipase on SPION-silica NPs in comparison with heating value of 42 MJ/kg for biodiesel indicates that biodiesel production through this method is unsustainable from the view point of energy. It is worth mentioning that this exergy balance is related to the coded zero condition (methanol to WCO molar ratio of 6, immobilized lipase concentration of 25%, water content of 12% and reaction time of 15 h as noted above), not at optimized conditions of the enzymatic transesterification of WCO. Optimization of the process can reduce heat and work demands as well as wastes resulting in reduction of internal and external exergy destroyed. Most of the unreacted substances (glycerides and FFA) are normally stored in tanks and then reused in the transesterification to increase the conversion to FAME, resulting in reduction of the mass input requirement and the waste fraction.<sup>32</sup> Technological choices through their performance differences also alter the results. For example, in the present work, the exergy consumed to produce 1 kJ of electricity was taken as 4.17 kJ, which is the value for fossil fuel based electricity generation.<sup>33</sup> If hydropower is used for electricity generation, the exergy cost reduces up to 0.006 kJ/kJ of electricity.<sup>34</sup> This would affect the exergy efficiency and the renewability indicator of the enzymatic transesterification process.

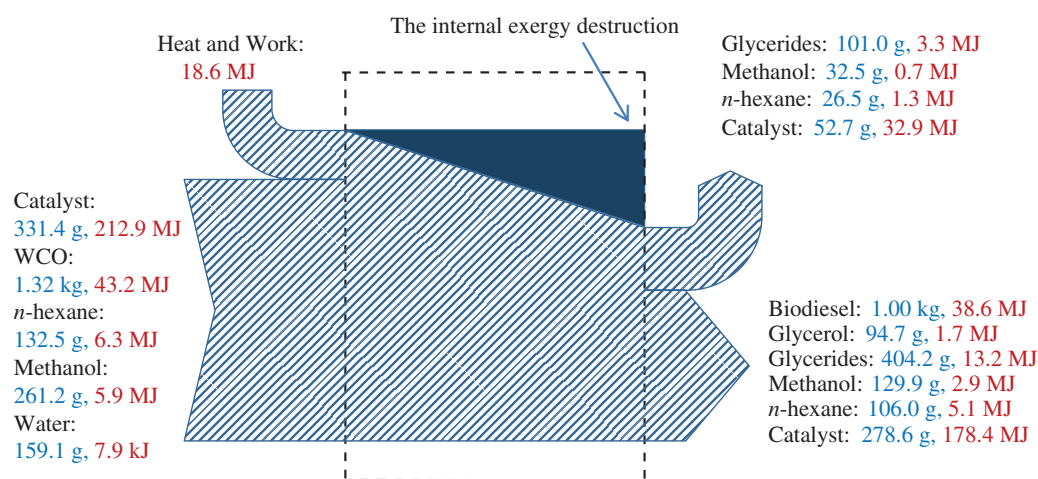


Figure 3. Simplified mass and exergy Sankey diagram for the enzymatic transesterification using immobilized lipase on SPION-silica NPs.

## Fitting the model by RSM

The complete design matrix and the results obtained for the FAME content and exergy efficiency of the enzymatic transesterification of WCO along with the corresponding points on the fitted models developed by RSM using the RCCD experimental design are summarized in Table 2. The model equation that correlates the FAME content of the enzymatic transesterification as the response to the experiment variables in terms of coded values is given as:

$$Y_1 = 74.35 + 0.99 m + 5.90 l + 0.69 w + 8.64 t - 1.36 m^2 - 2.26 l^2 - 0.95 l \times w + 1.27 l \times t - 1.35 w^2 - 0.87 t^2 \quad (15)$$

where  $Y_1$  is FAME content in the enzymatic transesterification (%),  $m$ ,  $l$ ,  $w$ , and  $t$  are molar ratio of methanol to WCO, weight percent of immobilized lipase to WCO, water content and reaction time, respectively. The statistical significance of the model developed by RSM was evaluated using ANOVA and summarized in Table 3. The model F-value of 124.58 and p-value of <.0001 indicated that the model of FAME content was statistically significant at a 95% confidence level ( $p < 0.05$ ). The model terms with  $p < 0.05$  were also significant in the model. The “lack of fit” of the model with low F-value of 1.07 and high p-value of 0.55 indicated that the model is not significant relative to the pure error, which was favorable for the model to fit. The determination coefficient ( $R^2$ ) was also used to evalu-

**Table 2. Experimental design matrix with FAME content and exergy efficiency from experiments and as predicted by RSM and ANN.**

Run	Coded process variables				Experimental data		Predicted data by RSM		Predicted data by ANN	
	Methanol to WCO (mol/mol)	Immobilized lipase concentration (wt.%)	Water content (wt.%)	Reaction time (h)	FAME content (%)	Exergy efficiency (%)	FAME content (%)	Exergy efficiency (%)	FAME content (%)	Exergy efficiency (%)
1	-1	-1	-1	-1	51.61	80.88	52.57	80.99	51.61	80.91
2	-1	-1	-1	1	68.00	77.37	67.40	77.39	67.96	77.49
3	-1	-1	1	-1	57.24	82.78	55.86	82.59	57.23	82.65
4	-1	-1	1	1	72.06	79.03	70.69	79.00	72.05	79.01
5	-1	1	-1	-1	63.43	81.11	63.77	81.03	63.43	81.13
6	-1	1	-1	1	82.84	79.31	83.68	79.33	82.84	79.25
7	-1	1	1	-1	63.80	81.88	63.27	81.70	63.80	81.90
8	-1	1	1	1	82.43	80.02	83.18	80.00	82.42	79.99
9	1	-1	-1	-1	54.56	81.12	54.56	81.18	54.54	81.19
10	1	-1	-1	1	70.74	77.61	69.39	77.59	70.73	77.75
11	1	-1	1	-1	59.53	82.94	57.85	82.79	59.50	82.82
12	1	-1	1	1	71.05	78.95	72.68	79.19	71.02	79.15
13	1	1	-1	-1	63.95	81.12	65.76	81.22	63.96	81.21
14	1	1	-1	1	86.58	79.47	85.67	79.53	86.55	79.55
15	1	1	1	-1	65.89	81.96	65.26	81.89	65.87	81.98
16	1	1	1	1	84.46	80.11	85.16	80.20	84.46	80.12
17	-2	0	0	0	66.52	80.09	66.95	80.18	66.56	80.28
18	2	0	0	0	70.76	80.82	70.93	80.57	70.82	80.70
19	0	-2	0	0	51.77	79.57	53.51	79.52	51.86	79.51
20	0	2	0	0	78.30	80.68	77.19	80.57	78.33	80.62
21	0	0	-2	0	68.24	79.42	67.60	79.20	68.27	79.22
22	0	0	2	0	69.14	81.40	70.39	81.47	69.20	81.56
23	0	0	0	-2	53.05	83.08	53.54	83.29	53.07	83.14
24	0	0	0	2	88.16	78.17	88.28	78.00	88.20	78.01
25	0	0	0	0	73.00	80.66	74.39	80.65	74.30	80.70
26	0	0	0	0	74.61	80.75	74.39	80.65	74.30	80.70
27	0	0	0	0	75.44	80.80	74.39	80.65	74.30	80.70



**Table 3. ANOVA of quadratic response surface models for FAME content and exergy efficiency.**

Term	FAME content					Exergy efficiency				
	Coefficient value	SE	SS	DF	<i>p</i> -value	Coefficient value	SE	SS	DF	<i>p</i> -value
Model			2844.02	10	<.0001			56.81	9	<.0001
Constant	-55.23					79.43				
<i>m</i>	17.34	0.2734	23.66	1	0.0022	0.898	0.0323	0.23	1	0.0073
<i>l</i>	1.63	0.2734	836.03	1	<.0001	0.029	0.0323	1.77	1	<.0001
<i>w</i>	2.78	0.2734	11.41	1	0.0227	0.406	0.0323	7.75	1	<.0001
<i>t</i>	2.14	0.2734	180.91	1	<.0001	-0.502	0.0323	41.97	1	<.0001
<i>m</i> <sup>2</sup>	-1.36	0.2901	39.57	1	0.0002	-0.067	0.0323	0.11	1	0.0547
<i>m</i> × <i>l</i>										
<i>m</i> × <i>w</i>										
<i>m</i> × <i>t</i>										
<i>l</i> <sup>2</sup>	-0.02	0.2901	109.27	1	<.0001	-0.002	0.0323	0.53	1	0.0002
<i>l</i> × <i>w</i>	-0.02	0.3349	14.42	1	0.0120	-0.006	0.0395	0.88	1	<.0001
<i>l</i> × <i>t</i>	0.03	0.3349	25.83	1	0.0016	0.010	0.0395	3.61	1	<.0001
<i>w</i> <sup>2</sup>	-0.08	0.2901	38.85	1	0.0003	-0.005	0.0323	0.14	1	0.0275
<i>w</i> × <i>t</i>										
<i>t</i> <sup>2</sup>	0.04	0.2901	16.17	1	0.0084					
Residual			28.72	16				0.42	17	
Lack of fit			25.64	14	0.5478			0.41	15	0.1642
Pure error			3.07	2				0.01	2	
Cor. total			2872.74	26				57.23	26	

ate the fitness of the model.  $R^2$  indicated that the model could explain 98.38% of the variability. Besides, a relatively low coefficient of variation value (CV=1.84%) implied a better precision and reliability of the experiments.<sup>19</sup> Hence, based on the high value of correlation and the low value of CV in the developed model by RSM, there is good agreement and precision between predicted and experimental values of the FAME content following enzymatic transesterification.

Multiple regression analysis of the experimental data also developed a second-order polynomial model based on coded units for exergy efficiency of the enzymatic transesterification of WCO using immobilized lipase on SPION-silica NPs as given in equation<sup>16</sup>:

$$Y_2 = 80.67 + 0.10 m + 0.27 l + 0.56 w - 1.32 t - 0.07 m^2 - 0.15 l^2 - 0.24 l \times w + 0.47 l \times t - 0.08 w^2 \quad (16)$$

where  $Y_2$  is the exergy efficiency of the enzymatic transesterification (%). Table 3 indicates the statistical significance of the model for the exergy efficiency evaluated by ANOVA. The regression model was highly significant, as is evident from the F-value of 150.32 and *p*-value of <.0001

for the exergy efficiency of the process. The large value of F implies that most of the variation in the response can be predicted by the regression equation. The *p*-value also estimates whether F is large enough to indicate statistical significance. In the developed model of exergy efficiency,  $R^2$  and CV were found to be 98.77 and 0.21 respectively. Apart from that, the 'Lack of Fit F-value' of 6.24 implies that lack of fit is not significant relative to pure error for the developed model.

### Interactions between process variables

The surface plots as the graphical representations of the regression equations related to the FAME content and exergy efficiency of the enzymatic transesterification of WCO using immobilized lipase on SPION-silica NPs are presented in Fig. 4. The effect of varying methanol to WCO molar ratio and catalyst concentration on the FAME content and exergy efficiency at constant water content of 12% and reaction time of 15 h is shown in Figs 4(a) and 4(b). Figure 4(a) indicates that both variables of methanol to WCO and catalyst concentration had significant effects on the FAME content. An increment in catalyst concentra-

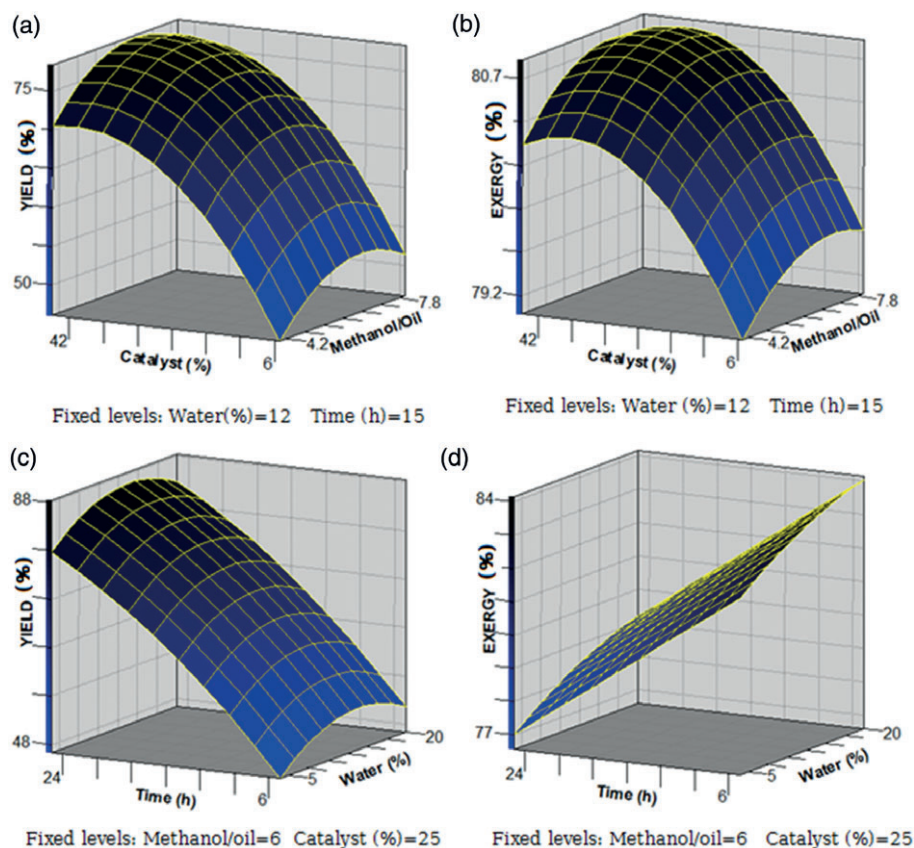


Figure 4. Surface plots of (a) FAME content (%) in terms of methanol to WCO molar ratio and catalyst concentration (%), (b) exergy efficiency (%) in terms of methanol to WCO molar ratio and catalyst concentration (%), (c) FAME content (%) in terms of water content (%) and reaction time (h), (d) exergy efficiency (%) in terms of water content (%) and reaction time (h).

tion caused an increase in the FAME content, so that the highest FAME content was obtained at the highest catalyst concentration. This phenomenon could be attributed to the increase in absorption of substrate molecules onto the active center of the lipase, with the more lipase available.<sup>35</sup> However the increase rate of FAME content declined as immobilized lipase content rose from 25% to 45%. The WCO content was excessive when catalyst concentration was under 25%, and that as the catalyst concentration rose to become sufficient from 25% to 45%, the FAME content increased only 4%.

Yaakob *et al.*<sup>36</sup> have recommended that due to the reversibility of the transesterification reaction, methanol to oil molar ratio should be used in an excess amount of the stoichiometric ratio (i.e., a molar ratio of methanol to oil of 3:1). Methanol is known as a lipase inhibitor and so high methanol content in the reaction can significantly inhibit lipase activity. Therefore, a step-wise methanol addition strategy is commonly applied.<sup>36</sup> As shown in

Fig. 4(a), the FAME content increased with increasing molar ratio of methanol to WCO to about 6, and then started to decrease when this ratio was further increased from 6 to 9. At molar ratios under 6 for the methanol to WCO, there was a positive interaction between methanol to WCO ratio and catalyst concentration on the WCO conversion to biodiesel. At the constant molar ratio of 6 for the methanol to WCO, the FAME content increased more strongly with an increase in catalyst concentration in comparison with the same increase in catalyst concentration and a methanol to WCO ratio of 4. In contrast, at molar ratios more than 6 for methanol to WCO ratio, a negative interaction was found between these factors. This means that in increasing the methanol ratio from 6 to 8, the positive effect of catalyst concentration on the WCO conversion to biodiesel was diminished.

From an exergy point of view, as shown in Fig. 4(b), the exergy efficiency increased with increasing both methanol to WCO molar ratio and catalyst concentration, followed

by a decline in efficiency when further increasing these factors. In calculating the exergy flow in the enzymatic production of biodiesel, a waste of 20% was assumed for recovery of outputs such as methanol and immobilized lipase. Therefore, waste of the least content of methanol and immobilized lipase was considerable to the extent that exergy waste of the least levels of these factors was more than the addition exergy of biodiesel produced through increasing FAME content caused by the factors. Therefore, adding more methanol and immobilized lipase than the optimum caused more exergy destruction and lower exergy efficiency. In the experiment condition with constant water content of 12% and reaction time of 15 h, the highest exergy efficiency occurred at a methanol to WCO molar ratio of 6 and immobilized lipase concentration of 28%.

The individual and cumulative effects of water content and reaction time on the FAME content are graphically represented in a 3D surface in Fig. 4(c). The FAME content increased gradually with an increase in the water content from 0% to 10% of WCO, and then declined as water content increased from nearly 10% to 20%. For the enzymatic transesterification of WCO in predominantly non-aqueous media, water plays multiple roles and has a strong influence on the catalytic activity and stability of the lipase.<sup>37</sup> Some water is essential to keep the enzyme active in organic solvents. However, water might take part in the enzymatic transesterification, thus influencing the equilibrium.<sup>38</sup> Water facilitates an increase in the available interfacial area, thus helping to maintain lipase activity. However, excess water might make the lipase more flexible and lead to some unintended side-reactions such as hydrolysis, especially in the transesterification process. As shown in Fig. 4(c), the FAME content increased along with the increase in the reaction time. However, with the increase in the reaction time, the rate of increase in the FAME content slightly decreased. The reaction rate was affected by mass transfer limitations.<sup>39</sup> The lower rates at the end of the reaction time might be due to insufficient mass transfer because of low mutual solubility of methanol and WCO, which is mainly due to the fact that glycerol is formed as reaction takes place, making solubility and mass transfer progressively limited.<sup>40</sup>

As can be seen in Fig. 4(d), the exergy efficiency steadily decreased with increasing reaction time. Although FAME content increased with time, exergy efficiency was observed only to decline with increasing reaction time. Heating and stirring of the reaction consumed electricity to accelerate WCO conversion to biodiesel, and electricity demand was nearly constant. Therefore, electricity

input steadily increased with increasing reaction time. With constant input, a reaction with high yield destroys a lower exergy through a lower waste of outputs. Therefore, an increase in FAME content could reduce exergy waste and enhance exergy efficiency provided that exergy input is constant or any increase in exergy input is lower than the corresponding increase in exergy output. But an increase in reaction time enhanced exergy demand more than exergy output by FAME content (or exergy saved through preventing destroyed exergy by material waste). However, the results show that the long reaction time in the enzymatic transesterification with correspondingly high exergy destruction can be considered as one of the main obstacles in development of biocatalysts in transesterification.

## Analysis by artificial neural networks

A variety of the architectures and topologies of neural networks were selected and tested for estimation and prediction of the FAME content and the exergy efficiency of enzymatic transesterification. Along with the learning algorithms, a variety of transfer functions were also tested for both output and hidden layers. The transfer function types employed in the neural network affect the ANN learning rate and aid its performance.<sup>20</sup> Several iterations were conducted with different numbers of neurons placed in the hidden layer to determine the optimal ANN structure to predict the output layer. It was started with two neurons and increased the number up to thirty. A self-organizing feature map network based on Bayesian regularization was finally selected as the best training algorithm to predict the process. The Multilayer Full Feed Forward with sigmoid connection type for the hidden layer and linear for the output layer, were employed in the ANN. The least MSE value and a good prediction of the outputs of both training and test sets were obtained with fourteen neurons in the hidden layer. The predicted values of the responses using the employed ANN are provided in Table 2. The predicted and actual values were employed to calculate  $R^2$  for both responses. Figure 5 shows the correlation between actual and predicted values based on the ANN model for both responses. As shown, the employed ANN improved  $R^2$  values in both cases as compared to RSM, which confirmed capability of ANN for fitting a reliable model with only 27 experimental points. The results showed that both RSM and ANN optimization tools gave good predictions due to the values of  $R^2$  and small values of MSE. However, ANN showed a clear superiority over RSM because of the higher values of  $R^2$  and

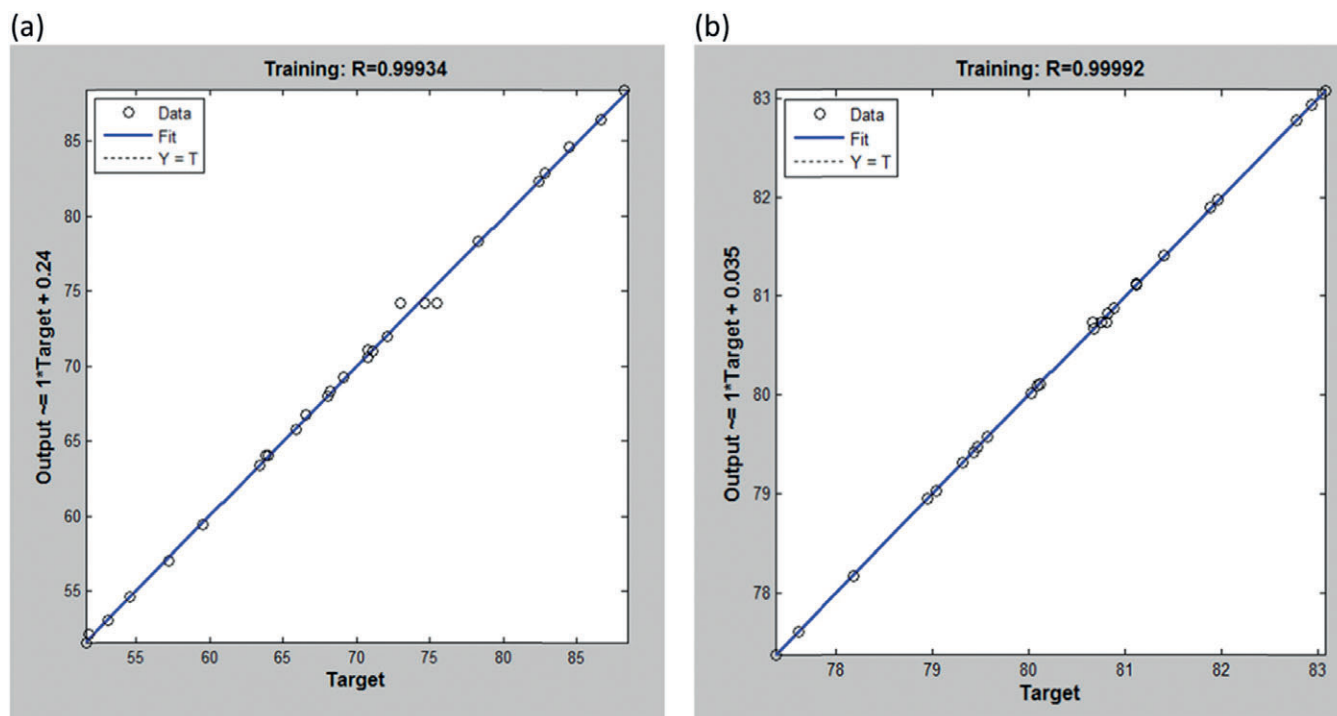


Figure 5. Correlation between experimental and predicted values by ANN for (a) FAME content and (b) exergy efficiency.

smaller values of MSE obtained. In addition, data fitting of the models were tested and the ANN models demonstrated a better fitting than RSM (Fig. 5). Therefore, it can be claimed that ANN was better than RSM in the modeling studies of the enzymatic transesterification.

## Optimization

By comparing the predicted and experimental values in both training and testing sets, it is not only shown that ANN has capability in predicting known data responses (the data that have been used for training) but also has the ability for generalization of unknown data along with responses into the range of experimental design (the data that have not been used for training). This implies that models developed by ANN can be used to adequately describe the output variables of FAME content and exergy efficiency of the enzymatic transesterification. The ANN trained in this study was used for predicting both responses (FAME content and exergy efficiency) in 160 000 ( $20 \times 20 \times 20 \times 20$ ) different simulated combinations of the four experiment variables (molar ratio of methanol to WCO, immobilized lipase concentration, water content and reaction time) that completely covered the experimental space. In the present work involving multiple responses, the acceptability of the process was depend-

ent on more than one response. In such situations the desirability of the process depends on the simultaneous optimization of two responses, FAME content and exergy efficiency of the enzymatic transesterification of WCO. Optimization was implemented by using the desirability profile and its function. Therefore, the values predicted by the ANN were used to calculate their  $d_k$  (desirability of response of  $k$ ) and  $D$  (overall desirability) values.<sup>41</sup>

For individual desirability of FAME content, the maximum value of this response based on optimization of the input space by DFA with data generated by ANN was obtained with FAME content as high as 95.7%. The design variables corresponding to the maximum objective function value, including methanol to WCO molar ratio, catalyst concentration, water content and reaction time, were set at 6.7, 45%, 9%, and 25 h, respectively. For individual desirability of exergy efficiency, the maximum value based on the developed DFA was found to be 84.6% at a methanol to WCO molar ratio of 8, catalyst concentration of 9%, water content of 12% and reaction time of 5 h. For simultaneous optimization of two responses, the maximum value for the overall desirability was found at a methanol to WCO molar ratio of 6.7, catalyst concentration of 35%, water content of 12% and reaction time of 20 h. The response values for FAME content and exergy efficiency that correspond to this combination were 88.6% and 80.1%, respectively.

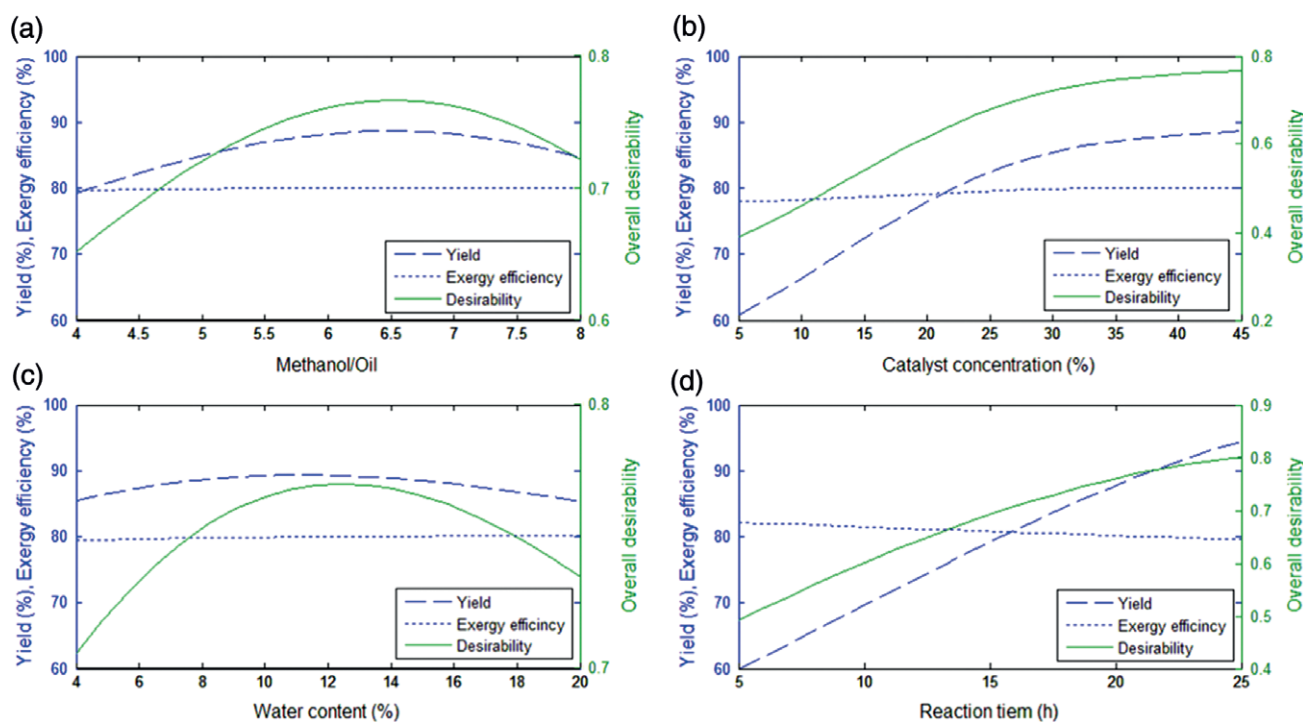


Figure 6. Effects of experimental variables on FAME content, exergy efficiency and overall desirability at the optimal points.

The effects of design variables in the enzymatic transesterification of WCO on FAME content, exergy efficiency and overall desirability as the objective functions at optimal points are shown in Fig. 6. In each plot displayed in the figure, the influence of one of the experiment variables on FAME content, exergy efficiency and overall desirability was depicted while holding the other factors constant at the optimal point. Among the experiment variables with the ranges studied in the present work, the catalyst concentration and reaction time were recognized as the most effective factors influencing biodiesel production and exergy efficiency. However, the reaction time of the experiments, even at the longest time of 25 h, was a limiting factor for biodiesel production but was also the main factor in exergy destruction during enzymatic transesterification. It is recommended that in order to develop biocatalysts for transesterification, the energy (electricity) demand of the reaction should be decreased by reducing the reaction time or by enhancing the energy efficiency with higher performance technologies such as microwave and ultrasound irradiation in the reaction.

## Conclusions

This study investigated the influence of FAME content and energy factors on the progress of waste cooking

oil (WCO) conversion to biodiesel catalyzed by immobilized lipase on SPION-silica NPs. The *T. lanuginosa* lipase was successfully immobilized onto magnetic mesoporous silica-SPION NPs and then used for enzymatic transesterification of WCO to synthesize biodiesel. Methanol to WCO molar ratio, catalyst concentration, water content and reaction time were considered as the main design variables and multi-objective functions including FAME content and exergy efficiency were proposed to achieve maximum desirability. Two quadratic response surface equations were successfully established by RSM to study the modeling and interaction of the variables for FAME content and exergy efficiency of the enzymatic transesterification using the experimental data based on RCCD methodology. A multiple input and output ANN was also developed for predicting and simultaneously optimizing the response based on a DFA. Based on individual desirability, a maximum FAME content of 95.7% was predicted at the methanol to WCO molar ratio of 6.7, catalyst concentration of 45%, water content of 9% and reaction time of 25 h while a maximum exergy efficiency of 84.6% occurred at a methanol to WCO molar ratio of 8, catalyst concentration of 9%, water content of 12% and reaction time of 5 h. FAME content by the enzymatic transesterification of WCO was shown to improve

significantly with process catalyst concentration and reaction time, which were both found to be the main factors of exergy destruction. The energetic waste associated with the recovery of excess methanol, as well as an increase in downstream FAME purification requirements, might hinder the use of excess methanol in trying to increase FAME content. The design variables set at the methanol to WCO molar ratio of 6.7, a catalyst concentration of 35%, a water content of 12% and a reaction time of 20 h were identified as the optimal condition to achieve maximum desirability with FAME content and exergy efficiency values of 88.6% and 80.1%, respectively. The methods described here are useful in order to optimize design variables under the multiple objectives of high yield and high process efficiency.

## Acknowledgments

We gratefully acknowledge Dr Majid Lashgari, Chair of the Department of Biosystem Engineering, Arak University and Dr Saeed Hamidi, President of Arak University who assisted and encouraged the lead author to keep doing research.

## References

- Khoobakht G, Najafi G and Karimi M, Optimization of operating factors and blended levels of diesel, biodiesel and ethanol fuels to minimize exhaust emissions of diesel engine using response surface methodology. *Applied Thermal Engineering* **99**:1006–1017 (2016).
- Karimi M, Keyhani A, Akram A, Rahman M, Jenkins B and Stroeve P, Hybrid response surface methodology-genetic algorithm optimization of ultrasound-assisted transesterification of waste oil catalysed by immobilized lipase on mesoporous silica/iron oxide magnetic core-shell nanoparticles. *Environ Technol* **34**(13–14):2201–2211 (2013).
- Lu J, Nie K, Xie F, Wang F and Tan T, Enzymatic synthesis of fatty acid methyl esters from lard with immobilized *Candida* sp. 99–125. *Process Biochem* **42**(9):1367–1370 (2007).
- Zhang Y, Dube M, McLean D and Kates M, Biodiesel production from waste cooking oil: 2. Economic assessment and sensitivity analysis. *Bioresour Technol* **90**(3):229–240 (2003).
- Xue F, Miao J, Zhang X, Luo H and Tan T, Studies on lipid production by *Rhodotorula glutinis* fermentation using monosodium glutamate wastewater as culture medium. *Bioresour Technol* **99**(13):5923–5927 (2008).
- Karimi M, Jenkins B and Stroeve P, Ultrasound irradiation in the production of ethanol from biomass. *Renew Sustain Energy Rev* **40**:400–421 (2014).
- Lara Pizarro AV and Park EY, Lipase-catalyzed production of biodiesel fuel from vegetable oils contained in waste activated bleaching earth. *Process Biochem* **38**(7):1077–1082 (2003).
- Lu J, Nie K, Wang F and Tan T, Immobilized lipase *Candida* sp. 99–125 catalyzed methanolysis of glycerol trioleate: Solvent effect. *Bioresour Technol* **99**(14):6070–6074 (2008).
- Cao L, Immobilised enzymes: science or art? *Curr Op Chem Biol* **9**(2):217–226 (2005).
- Salis A, Pinna M, Monduzzi M and Solinas V, Comparison among immobilised lipases on macroporous polypropylene toward biodiesel synthesis. *J Molec Catal B* **54**(1):19–26 (2008).
- Tonon S, Brown M, Luchi F, Mirandola A, Stoppato A and Ulgiati S, An integrated assessment of energy conversion processes by means of thermodynamic, economic and environmental parameters. *Energy* **31**(1):149–163 (2006).
- Yang Q, Chen B, Ji X, He Y and Chen G, Exergetic evaluation of corn-ethanol production in China. *Communications in Nonlinear Science and Numerical Simulation* **14**(5):2450–2461 (2009).
- Khoobakht G, Akram A, Karimi M and Najafi G, Exergy and energy analysis of combustion of blended levels of biodiesel, ethanol and diesel fuel in a DI diesel engine. *Appl Therm Eng* **99**:720–729 (2016).
- Ojeda K and Kafarov V, Exergy analysis of enzymatic hydrolysis reactors for transformation of lignocellulosic biomass to bioethanol. *Chem Eng J* **54**(1):390–395 (2009).
- Fermin WJ and Corzo O, Optimization of vacuum pulse osmotic dehydration of cantaloupe using response surface methodology. *Journal of Food Processing and Preservation* **29**(1):20–32 (2005).
- Garrote RL, Coutaz VR, Luna JA, Silva ER and Bertone RA, Optimizing processing conditions for chemical peeling of potatoes using response surface methodology. *J Food Sci* **58**(4):821–826 (1993).
- Corzo O and Gomez ER, Optimization of osmotic dehydration of cantaloupe using desired function methodology. *J Food Eng* **64**(2):213–219 (2004).
- Guillou AA and Floros JD, Multiresponse optimization minimizes salt in natural cucumber fermentation and storage. *J Food Sci* **58**(6):1381–1389 (1993).
- Karimi F, Rafiee S, Taheri-Garavand A and Karimi M, Optimization of an air drying process for *Artemisia absinthium* leaves using response surface and artificial neural network models. *Journal of the Taiwan Institute of Chemical Engineers* **43**(1):29–39 (2012).
- Betiku E and Ajala SO, Modeling and optimization of *Thevetia peruviana* (yellow oleander) oil biodiesel synthesis via *Musa paradisiacal* (plantain) peels as heterogeneous base catalyst: A case of artificial neural network vs. response surface methodology. *Ind Crop Prod* **53**:314–322 (2014).
- Bringas E, Köysüren Ö, Quach DV, Mahmoudi M, Aznar E, Roehling JD *et al.*, Triggered release in lipid bilayer-capped mesoporous silica nanoparticles containing SPION using an alternating magnetic field. *Chem Comm* **48**(45):5647–5649 (2012).
- Ting W-J, Tung K-Y, Giridhar R and Wu W-T, Application of binary immobilized *Candida rugosa* lipase for hydrolysis of soybean oil. *J Molec Catal B* **42**(1):32–38 (2006).
- Xie W and Wang J, Immobilized lipase on magnetic chitosan microspheres for transesterification of soybean oil. *Biomass Bioenergy* **36**:373–380 (2012).
- Chen Y, Xiao B, Chang J, Fu Y, Lv P and Wang X, Synthesis of biodiesel from waste cooking oil using immobilized lipase in fixed bed reactor. *Energy Convers Manage* **50**(3):668–673 (2009).
- Szargut J, Chemical exergies of the elements. *Appl Energy* **32**(4):269–286 (1989).

26. Jaimes W, Acevedo P and Kafarov V, Exergy analysis of palm oil biodiesel production. *Chem Eng* **21**:1345–1350 (2010).
27. Peralta-Ruiz Y, González-Delgado A-D and Kafarov V. Evaluation of alternatives for microalgae oil extraction based on exergy analysis. *Appl Energy* **101**:226–236 (2013).
28. Blanco-Marigorta A, Suárez-Medina J and Vera-Castellano A, Exergetic analysis of a biodiesel production process from *Jatropha curcas*. *Appl Energy* **101**:218–225 (2013).
29. Hu Z, Cai M and Liang H-H, Desirability function approach for the optimization of microwave-assisted extraction of saikosaponins from *Radix Bupleuri*. *Separ Purif Technol* **61**(3):266–275 (2008).
30. Ofori-Boateng C, Keat TL and JitKang L, Feasibility study of microalgal and *jatropha* biodiesel production plants: Exergy analysis approach. *Appl Therm Eng* **36**:141–151 (2010).
31. Pierre P, *A to Z of Thermodynamics*. Oxford Oxford University Press, Oxford (1998).
32. Talens L, Villalba G and Gabarrell X, Exergy analysis applied to biodiesel production. *Resourc Conserv Recy* **51**(2):397–407 (2007).
33. Sorguven E and Äzilgen M, Thermodynamic assessment of algal biodiesel utilization. *Renew Energy* **35**(9):1956–1966 (2010).
34. Berthiaume R, Bouchard C and Rosen MA, Exergetic evaluation of the renewability of a biofuel. *Exergy, An International Journal* **1**(4):256–268 (2001).
35. Bhattacharya S and Banerjee R, Laccase mediated biodegradation of 2, 4-dichlorophenol using response surface methodology. *Chemosphere* **73**(1):81–85 (2008).
36. Yaakob Z, Mohammad M, Alherbawi M, Alam Z and Sopian K, Overview of the production of biodiesel from Waste cooking oil. *Renew Sustain Energy Rev* **18**:184–193 (2013).
37. Lu J, Chen Y, Wang F and Tan T, Effect of water on methanolysis of glycerol trioleate catalyzed by immobilized lipase *Candida* sp. 99–125 in organic solvent system. *J Molec Catal B* **56**(2):122–125 (2009).
38. Kaieda M, Samukawa T, Matsumoto T, Ban K, Kondo A, Shimada Y *et al.*, Biodiesel fuel production from plant oil catalyzed by *Rhizopus oryzae* lipase in a water-containing system without an organic solvent. *J Biosci Bioeng* **88**(6):627–631 (1999).
39. Yu D, Tian L, Wu H, Wang S, Wang Y, Ma D, *et al.*, Ultrasonic irradiation with vibration for biodiesel production from soybean oil by Novozym 435. *Process Biochem* **45**(4):519–525 (2010).
40. Batistella L, Lerin LA, Brugnerotto P, Danielli AJ, Trentin CM, Popielski A *et al.*, Ultrasound-assisted lipase-catalyzed transesterification of soybean oil in organic solvent system. *Ultrason Sonochem* **19**(3):452–458 (2012).
41. Giordano PC, Martínez HD, Iglesias AA, Beccaria AJ and Goicoechea HC, Application of response surface methodology and artificial neural networks for optimization of recombinant *Oryza sativa* non-symbiotic hemoglobin 1 production by *Escherichia coli* in medium containing byproduct glycerol. *Bioresour Technol* **101**(19):7537–7544 (2010).



### Mahmoud Karimi

Mahmoud Karimi is Assistant Professor of Biosystems Engineering at Arak University, Iran. He has been with Department of Chemical Engineering, UC Davis, USA, in 2012 and is currently in the Department of Chemistry at Stanford University, as a researcher.

His researches lie at the interface of energy and environment, with a focus on sustainable development in bioenergy. He conducts researches in bioprocess engineering in bioenergy, biomass conversion, biofuel production, thermodynamic analysis and life cycle assessment. He holds BSc Biosystems Engineering from the University of Chamran, Iran, MSc and PhD Biosystems Engineering from University of Tehran, Iran.



### Pieter Stroeve

Pieter Stroeve is a distinguished professor in the UC Davis Department of Chemical Engineering. Stroeve's research covers multiple regions of chemical engineering; he explores colloid and surface science, self-assembled monolayers, supramolecular structures on surfaces, nanotechnology, lithium ion

batteries and membrane separations. He has created nanostructured surfaces of nanofibers, nanotubes and nanocables, and applied these breakthroughs to thermoelectrics and photovoltaic systems.



### Bryan Jenkins

Bryan Jenkins is Professor and Chair of Biological and Agricultural Engineering at the University of California, Davis. He teaches and conducts research in the areas of energy and power, with emphasis on biomass and other renewable resources. His research also

includes analysis and optimization of energy systems. He is a recipient of an Outstanding Achievement Award from the US Department of Energy for exceptional contributions to the development of bioenergy, and the Linneborn Prize from the European Union for outstanding contributions to the development of energy from biomass.